# Experimental Investigation of Low Frequency Noise Reduction Using a Nonlinear Vibroacoustic Absorber

Sergio Bellizzi, Bruno Cochelin, Philippe Herzog, Pierre-Olivier Mattei, Cédric Pinhède

**Proceedings of the ASME 2011 International Design Engineering Technical Conferences & Computers and Information in Engineering Conference**
**IDETC/CIE 2011**
**August 28-31, 2011, Washington, DC, USA**

**DETC2011-47431**

# EXPERIMENTAL INVESTIGATION OF LOW FREQUENCY NOISE REDUCTION USING A NONLINEAR VIBROACOUSTIC ABSORBER

**Sergio Bellizzi***
Laboratoire de Mécanique et d'Acoustique - CNRS
Marseille, France, 13402
bellizzi@lma.cnrs-mrs.fr

**Bruno Cochelin**
Laboratoire de Mécanique et d'Acoustique - CNRS
Ecole Centrale de Marseille
Marseille, France, 13451
bruno.cochelin@centrale-marseille.fr

**Philippe Herzog**
**Pierre-Olivier Mattéi**
**Cédric Pinhède**
Laboratoire de Mécanique et d'Acoustique - CNRS
Marseille, Fance, 13402
{herzog, mattei, pinhede}@lma.cnrs-mrs.fr

## ABSTRACT

*This work deals with the energy pumping phenomenon for acoustical applications. The concept of energy pumping is to passively reduce the vibrations of a primary system by attaching to it an essentially nonlinear damped oscillator also named Nonlinear Energy Sink (NES) creating a strongly nonlinear coupling which localizes and dissipates the vibrational energy. In the context of acoustics, a vibroacoustic coupling is used. In an earlier work, we showed experimentally that a loudspeaker used as a Suspended Piston (SP) working outside its range of linearity can be used as a NES. In this work, the performance and efficiency of a SP NES is studied numerically and experimentally. The considered acoustic medium is a resonant pipe. The coupling between the pipe and the NES is ensured acoustically by a small acoustic compliance (the air in a coupling box).Various observed aspects of energy pumping are presented: behavior under sinusoidal forcing, pumping threshold, resonance capture and transient response. As a SP NES technology permits an easy control of the moving mass of the NES, the effect of this parameter is also studied.*

## INTRODUCTION

During the last ten years, the Targeted Energy Transfer (TET) approach to passively control the vibrations of mechanical systems subjected to external inputs has been proposed and extensively studied. This approach represents a concept in which a strongly purely nonlinear, passive, local attachment, the Nonlinear Energy Sink (NES), is employed to alter (in the reduction sense) the dynamics of the primary system to which it is attached. This concept involves energy interactions which occur due to internal resonances making possible irreversible nonlinear energy transfers from the primary system to the NES component. In other words, the nonlinear substructure is introduced to couple the modes of the system introducing localized modes which are not excited directly. A complete description of the TET can be found in the monograph [1]. Some applications are reported in [2] [3].

In the context of noise reduction, the TET is a good opportunity to develop passive control device efficient at low frequencies. The first experimental evidence of TET in acoustics has been presented in [4]. The primary system was an acoustic medium and the NES was a thin visco-elastic membrane which was subjected to very large oscillations. A complete experimental study can be found in [5]. More recently, it was shown that a loudspeaker used as a suspended piston working outside its range of linearity can also be used as a NES [6]. The main advantage of the "suspended piston technology" versus "membrane technology" is the perspective to adjust independently the device parameters as the moving mass or the damping which are, as shown for example in [5], two of the most influent parameters of the

*Address all correspondence to this author.

NES.

The present study is the continuation of the numerical and experimental developments reported in [6]. This papers aims to experimentally verify the efficiency of employing a SP NES as a low frequency noise reduction in terms of transient responses, forced responses under sinusoidal forcing, pumping threshold and resonance capture. As a SP NES technology permits an easy control of the moving mass of the NES, the effect of this parameter is also reported.

## EXPERIMENTAL FIXTURE

The experimental fixture considered in this work to investigate the efficiency of a SP NES to low frequency noise reduction is depicted in Fig 1. It consists of a acoustic medium connected to a SP NES by means of a coupling box.

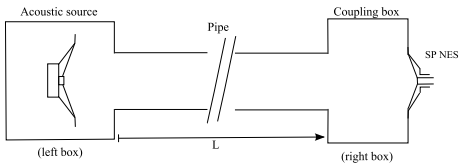


**FIGURE 1**. SKETCH OF THE EXPERIMENTAL FIXTURE.

### Acoustic Medium

The acoustic medium is composed by a straight pipe of length $L$ and section area $S_p$ (acoustic resonator) with two cubic boxes one at each end. The left box (volume $V_1$) is used as an acoustic source to excite the pipe. It is connected to the entrance of the pipe and it includes a Audax HT240GO loudspeaker which is fixed to the box using four rigid bindings (see Fig. 2). The configuration of the loudspeaker inside the box has been chosen to ensure a low coupling between the loudspeaker membrane and the pipe, avoiding the pipe damping by the loudspeaker. The right box (volume $V_2$) is connected to the end of the pipe at one of its sides and the SP NES is fixed on the opposite side. The air inside the box ensures the acoustical coupling between the tube and the SP NES. The two boxes were designed so that the acoustic behavior of the pipe is close to that of an open-open wave guide.

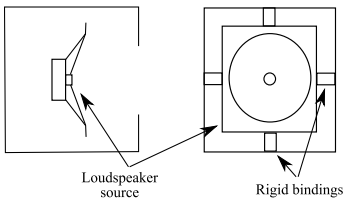


**FIGURE 2**. SKETCH OF ACOUSTIC SOURCE (including a front view (right)).

### NES Description

The SP NES is built from a commercial model of loudspeaker by suppressing the motor assembly. The SP NES consists of a structure including the diaphragm and the dust cap fixed to the rigid basket and supported by the spider. The nonlinear effect of the SP NES is based on geometrical nonlinearity induced by the large motion of the diaphragm. The behavior of the SP NES can be modeled as one Degree Of Freedom (DOF) system consisting as a mass supported by a nonlinear stiffness and including a low damping element assumed here viscous and linear (see Fig. 3). Compared to a thin visco-elastic membrane, one of the interests to use such a structure as a NES is that it is easy to modify some of its mechanical properties. This is the case for the moving mass of the NES which can be increased by adding a mass on the dust cap.

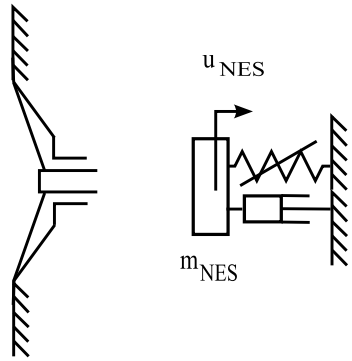


**FIGURE 3**. SKETCH OF THE SP NES (left) AND EQUIVALENT 1 DOF SYSTEM (right).

In this work, we have used the same SP NES as in [6]. It was built from an old AUDAX loudspeaker. The behavior of the SP NES was investigated experimentally using quasi-static and dynamic tests giving a representative one DOF nonlinear spring-damped-mass system. All this work is reported in [6].

### Dimensional and Adimensional Models

Following [5] and [6] and under the same assumptions, a simple model to predict qualitatively the behavior of the experimental fixture can be obtained corresponding to the following

equations of motion

$$m_a\ddot{u}_a(t) = -c_p\dot{u}_a(t) - k_p u_a(t) - S_p p_c(t) + S_p p_s(t), \quad (1)$$

$$m_{NES}\ddot{u}_{NES}(t) = -c_{NES}\dot{u}_{NES}(t) - \sum_{i=1}^{n_{NL}} k_{NES,i}\, u_{NES}(t)^i - S_{NES} p_c(t). \quad (2)$$

In Eq. (1), the quantities $m_a = \frac{\rho_a S_p L}{2}$, $k_p = \frac{\pi^2 c_0^2 \rho_a S_p}{2L}$ and $c_p$ represent the mass, the stiffness and damping of the 1-DOF system modeling the half-wavelength resonance of the pipe where $\rho_a$ denotes the density of the air and $c_0$ the sound wave velocity. $u_a(t)$ denotes the displacement of the air at the right end of the tube ($x = L$) assuming an axial distribution corresponding to the first mode of the tube (i.e $U_a(x,t) = u_a(t)\cos(\frac{\pi x}{L})$). This displacement is proportional to the acoustic pressure $p_p(t)$ at the middle axial position in the tube accordingly to the relationship

$$u_a(t) = -\frac{L}{\pi \rho_a c_0^2} p_p(t). \quad (3)$$

The acoustic source is modeled as an ideal pressure source, $p_s(t)$, acting at the left end of the pipe. In case of a sinusoidal excitation, the acoustic pressure reads as $p_s(t) = a_s \sin(\omega_s t)$.

In Eq. (2), the quantities $m_{NES}$, $c_{NES}$ and the coefficients $k_{NES,i}$ for $i = 1, \cdots, n_{NL}$ represent the mass, damping and the nonlinear stiffness of the 1-DOF system modelling the behaviour of the SP NES. The parameter values were obtained in [6].

The vibroacoustic coupling between the two subsystems is given by the acoustic pressure $p_c(t)$ into the coupling box which is related to $u_a(t)$ and $u_{NES}(t)$ accordingly to

$$p_c(t) = \frac{\rho_a c_0^2}{V_2}(S_p u_a(t) - \frac{S_{NES}}{2} u_{NES}(t)) \quad (4)$$

where $S_{NES}$ denotes the equivalent section area of the SP NES.

The numerical values of the parameters characterizing the experimental fixture are given hereafter in terms of geometrical quantities of the acoustic medium: $L = 3.85$ m, $S_p = 0.045$ m$^2$, $V_1 = 0.38$ m$^3$, $V_2 = 0.28$ m$^3$, in terms of damping ratio of the acoustic medium: $\tau_p = 0.01$ ($c_p = 2\tau_p\sqrt{m_a k_p}$), in terms of geometrical quantity of the SP NES: $S_{NES} = 0.0254$ m$^2$ and in terms of the mechanical quantities of the SP NES: $c_{NES} = 0.37$ kg/s, $m_{NES} = 0.012$ kg, $n_{NL} = 5$, $k_{NES,1} = 235$ N/m, $k_{NES,2} = -1970$ N/m$^2$, $k_{NES,3} = 2 \times 10^7$ N/m$^3$, $k_{NES,4} = 1.09 \times 10^9$ N/m$^4$, $k_{NES,5} = 6.5 \times 10^{10}$ N/m$^5$. The mass value $m_{NES} = 0.012$ kg corresponds to the nominal SP NES. This value can be increased by adding mass to the moving mass of the SP NES.

**TABLE 1**. PARAMETER VALUES OF THE ADIMENSIONAL MODEL (for $m_{NES} = 0.012$ and $d = 0.008555$ giving $\alpha_{2,3} = 1$).

| $\beta$ | $\gamma$ | $\mu_1/10$ | $\mu_2/10$ | $\alpha_{2,1}$ | $\alpha_{2,2}$ | $\alpha_{2,4}$ | $\alpha_{2,5}$ |
|---|---|---|---|---|---|---|---|
| 0.125 | 0.67 | 0.20 | 0.722 | 0.16 | -0.011 | 0.47 | 0.24 |

Introducing the following adimensional quantities and time normalization

$$u_1 = \frac{2S_p}{S_{NES}}\frac{u_a}{d},\ u_2 = \frac{u_{NES}}{d} \text{ and } \tau = \omega t \text{ with } \omega^2 = \frac{k_p}{m_a} \quad (5)$$

where $d$ is a characteristic length of the experiment ($d$ has to be chosen), the equations of motion Eqs. (1)(2) reads now (here we have assumed that the acoustic source is sinusoidal)

$$\ddot{u}_1 + \mu_1\dot{u}_1 + u_1 + \beta(u_1 - u_2) = F\sin(\Omega\tau) \quad (6)$$

$$\gamma\ddot{u}_2 + \mu_2\dot{u}_2 + f(u_2) + \beta(u_2 - u_1) = 0 \quad (7)$$

where

$$\beta = \frac{2S_p L}{\pi^2 V_2},\ \mu_1 = \frac{2c_p}{\pi c_0 \rho_a S_p},\ \gamma = \frac{4S_p m_{NES}}{\rho_a L S_{NES}^2},\ \mu_2 = \frac{4S_p c_{NES}}{\pi c_0 \rho_a S_{NES}^2}, \quad (8)$$

$$f(u_2) = \sum_{i=1}^{n_{NL}} \alpha_{2,i}\, u_2^i \text{ with } \alpha_{2,i} = \frac{4S_p L d^{i-1}}{\pi^2 c_0^2 \rho_a S_{NES}^2} k_{NES,i}, \quad (9)$$

$$F = \frac{4L}{\pi^2 c_0^2 \rho_a S_{NES} d} S_p a_s, \text{ and } \Omega = \frac{\omega}{\omega_s}. \quad (10)$$

It is interesting to note that the parameters $\beta$, $\mu_1$, $\gamma$ and $\mu_2$ do not depend on the length parameter $d$. Moreover, $\gamma$ is the only parameter depending on the NES mass $m_{NES}$.

The numerical values of the parameters of the adimensional model are given Tab. 1. These values correspond to $m_{NES} = 0.012$ and the length parameter $d$ has been chosen such that $\alpha_{2,3} = 1$.

## NUMERICAL INVESTIGATIONS

The objective of this section is to investigate the behavior of the system (6)(7) in terms of Nonlinear Normal Modes

(NNM) and forced responses under sinusoidal excitation. The free software ManLab [7] was used as numerical tool. The NNM and the forced responses including stability analysis are obtained combining the harmonic balance method (HBM) [8] [9] and the so-called Asymptotic Numerical Method (ANM) [10]. In this method the number of harmonics $H$ has to be chosen carefully. All the numerical results were obtained using $H = 7$. We checked that all the curves were only very slightly modified by increasing $H$ from 7 to 9.

The NNMs are one of the characteristics of a nonlinear dynamical system that can be used to analyze the nonlinear targeted energy transfer [1]. The NNMs are defined from the undamped ($\mu_1 = \mu_2 = 0$) and autonomous ($F = 0$) associated system. Fig. 4 shows the classical Frequency-Energy Plot (FEP) of the NNMs of the adimensional system for $\gamma = 0.67$ and $\gamma = 1.25$. The value $\gamma = 1.25$ corresponds to a SP NES with $m_{NES} = 0.022$ kg. FEP can be used to analyze free responses or responses under impulsive external forces. The dotted curves correspond to the NNM, named NNM$_{NES}$, starting, a low energy level, on the first linearized normal mode corresponding to the nonlinear component (the NES component). The continuous curves correspond to the NNM, named NNM$_{linear}$, starting, a low energy level, on the second linearized normal mode corresponding to the linear component. These curves look like the curves obtained with a cubic nonlinear restoring force. An estimate of pumping threshold in terms of energy

$$\text{Energy} = \frac{v_1^2}{2} + \gamma\frac{v_2^2}{2} + \frac{u_1^2}{2} + \beta\frac{(u_1-u_2)^2}{2} + \alpha_{2,1}\frac{u_2^2}{2} + \alpha_{2,2}\frac{u_2^3}{3} + \alpha_{2,3}\frac{u_2^4}{4} + \alpha_{2,4}\frac{u_2^5}{5} + \alpha_{2,5}\frac{u_2^6}{6} \qquad (11)$$

where $v_i = \dot{u}_i$, is given by the points $A_{Energy}$ and $B_{Energy}$ on the $NNM_{linear}$ branches showing that the pumping threshold increases with the mass value of the SP NES (starting from 0.968 for $m_{NES} = 0.012$ to 9.82 for $m_{NES} = 0.022$).

Another appropriate graphical depictions of the NNMs are the RMS-Frequency Plots (RFPs) where the amplitudes of the components ($u_1$ and $u_2$) in term of the Root-Mean-Square (RMS) of a periodic function are plotted as a function of the frequency. Fig. 5 shows the associated RFPs of the two NNMs shown Fig. 4 for $\gamma = 0.67$ (grey curves) and $\gamma = 1.25$ (black curves). As in Fig. 4, the continuous curves correspond to the NNM$_{linear}$ whereas the dashed curves correspond to the NNM$_{NES}$. For each mode two curves are plotted, one associated to the linear component $u_1$ and the other associated to the nonlinear component $u_2$. Here also, the pumping threshold can be estimated from the points $A_{RMS}$ and $B_{RMS}$ (on the $u_1$-branches of the NNM$_{linear}$) but now in terms of the RMS values of the periodic responses. As in the case of energy, the pumping threshold increases with the mass value of the SP NES (starting from 0.865 for $m_{NES} = 0.012$ to 2.88 for $m_{NES} = 0.022$).

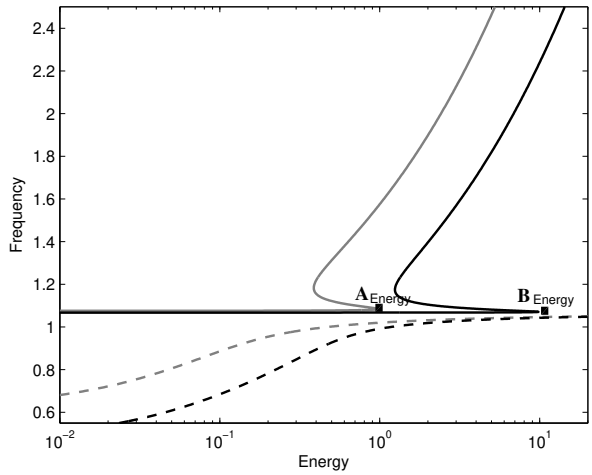


**FIGURE 4**. SIMULATION RESULTS. Frequency-energy plot of the two NNMs (NNM$_{linear}$, NNM$_{NES}$) of the adimensionel systems with $\gamma = 0.67$ (grey curves) and $\gamma = 1.25$ (black curves): NNM$_{linear}$ (continuous lines), NNM$_{NES}$ (dashed curves).

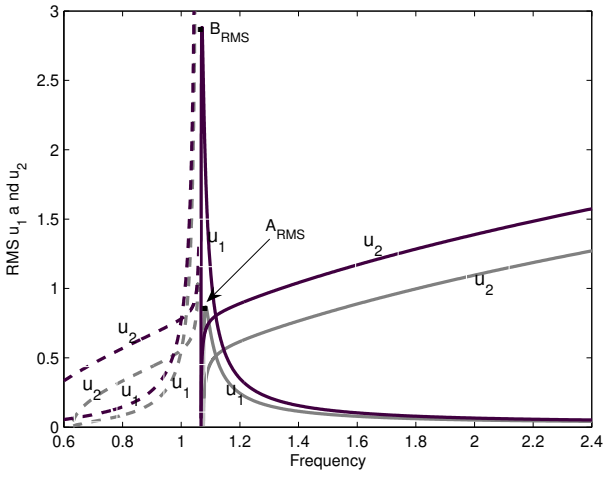


**FIGURE 5**. SIMULATION RESULTS. RMS-frequency plots of the two NNMs (NNM$_{linear}$, NNM$_{NES}$) of the adimensionel systems with $\gamma = 0.67$ (grey curves) and $\gamma = 1.25$ (black curves): NNM$_{linear}$ (continuous lines), NNM$_{NES}$ (dashed curves).

We now focus on the periodic responses of the complete system (6)(7) under sinusoidal excitations. Figs. 6 and 7 show the

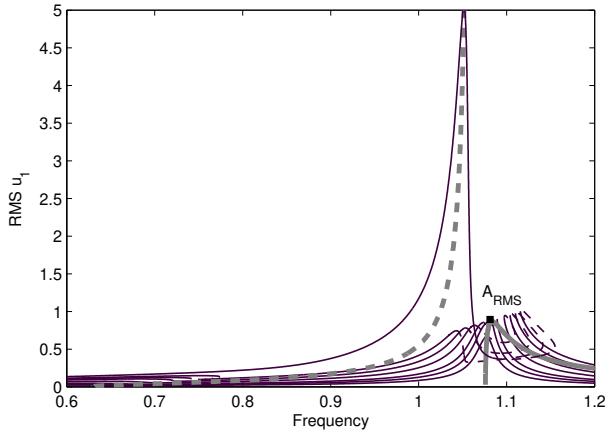


**FIGURE 6**. SIMULATION RESULTS. RMS values of the linear component $u_1$ of the periodic responses versus the excitation frequency for seven excitation level $F = 0.02, 0.03, 0.04, 0.06, 0.08, 0.1, 0.12$ (black curves). The RFPs of $u_1$ (grey curves) are also reported. (Here $\gamma = 0.67$).

RMS values of the linear component $u_1$ of the periodic responses versus the excitation frequency for seven excitation amplitudes $F = 0.02, 0.03, 0.04, 0.06, 0.08, 0.1$ and $0.12$. The zones of existence of unstable periodic responses are indicated as dashed curves. When the excitation level increases, a zone including instable periodic responses appears. This zone appears when the RMS value of the component $u_1$ becomes greater than the pumping threshold (see the curve number 2 and the grey curve on Fig. 7). Moreover, when the excitation level increases, the resonance shifts from the RFP of $u_1$ of the NNM$_{linear}$ to the RFP of $u_1$ of the NNM$_{NES}$.

The same comments can be made from Fig. 8 on the component $u_2$ except the influence of the pumping threshold.

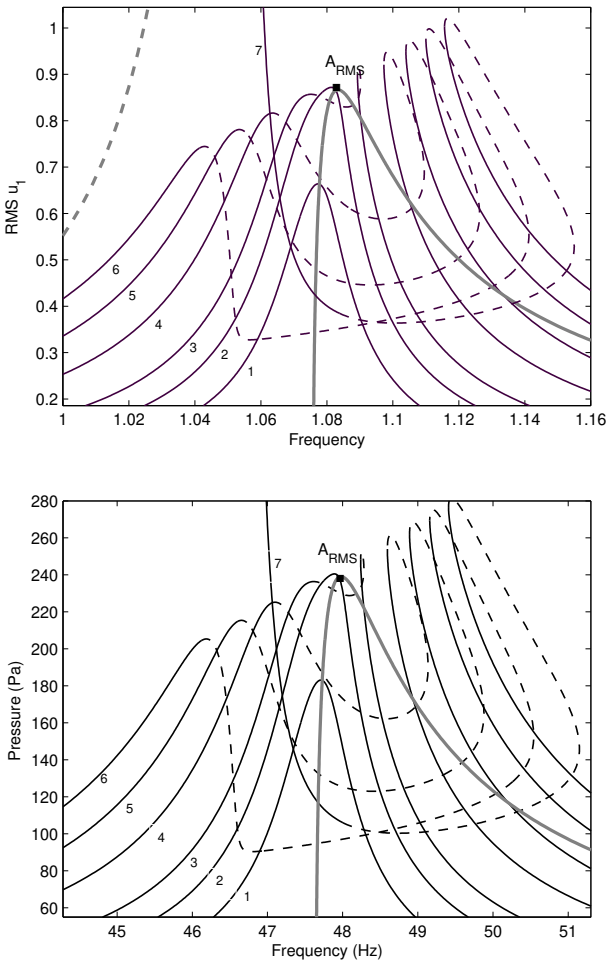


**FIGURE 7**. SIMULATION RESULTS. Zoom onto Fig. 6 for adimensional (top) and for the associated dimensional quantities (botton).

## EXPERIMENTAL INVESTIGATIONS

The tests were performed by exciting the tube by means of an acoustic source powered by an harmonic voltage signal $A_s \sin(2\pi f_s t)$ provided by a loudspeaker (see Fig. 2). The power amplifier (InterM R150) driving the loudspeaker was operated in voltage-feedback mode. During a test, the following responses were measured: the current and the voltage fed to the loudspeaker, the acoustic pressure at the middle section of the pipe by means of a microphone (GRAS, 40BH) and the velocity of the diaphragm of the SP NES by means of a laser vibrometer (Polytec, OFV303). A multi-channel analyzer/recorder (OROS OR38) including a signal generator was used with a sampling frequency of 4096 Hz.

We first report some free oscillations observed experimentally. In order to store the initial energy in the system, a sinusoidal excitation at a frequency close to the first resonance frequency of the pipe is applied. Then the excitation is stopped and the free responses are recorded. We first consider the SP NES without added mass. Fig. 9 shows the free responses in terms of acoustic pressure in the pipe and velocity of the SP NES initiated with a sinusoidal excitation ($f_s = 46.5$ Hz) for three different excitation amplitudes. To facilitate the comparison, the velocity and pressure amplitudes are scaled similarly. At low excitation level, the acoustic pressure and the velocity are out of phase and the sound extinction in the pipe follows a natural exponential decrease. When the excitation level increases, we observe that the acoustic pressure and the velocity start first in phase and then the motions become out of phase. The pumping occurs in the first phase and this phase is associated to a sound extinction much

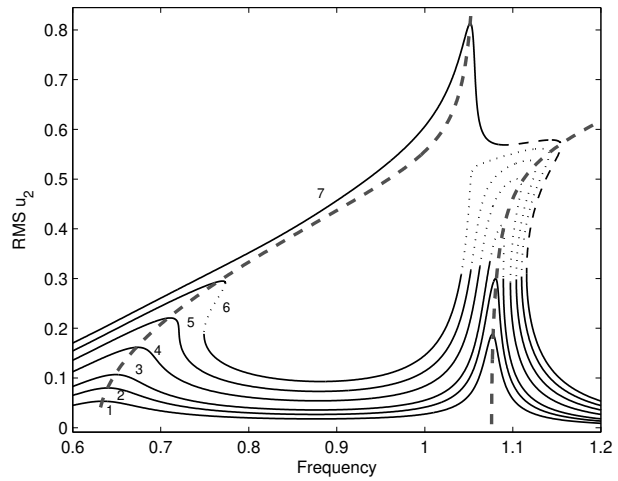


**FIGURE 8**. SIMULATION RESULTS. RMS values of the linear component $u_2$ of the periodic responses versus the excitation frequency for seven excitation level $F = 0.02, 0.03, 0.04, 0.06, 0.08, 0.1, 0.12$ (black curves). The RFPs of $u_2$ (grey curves) are also reported. (Here $\gamma = 0.67$).

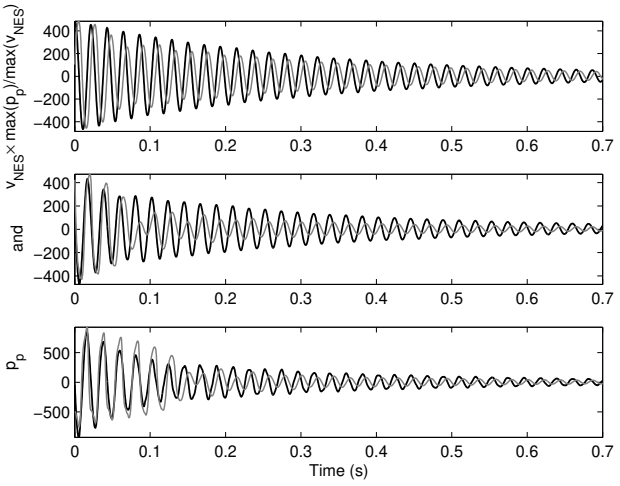


**FIGURE 9**. EXPERIMENTAL RESULTS. Configuration with SP NES without mass. Time series of the pressure in the pipe (black curves) and the velocity of the diaphram of the SP NES (grey curves). Initial condition associated to the sinusoidal excitation $f_s = 46.5$ Hz. low level (top), medium level (middle) and high level (bottom)

faster than the exponential one. Finally, the end of the pumping phase appears for the same level of the acoustic pressure.

We consider now the SP NES without and with an added mass (3 g). Fig. 10 shows for the almost same initial condition (associated to the sinusoidal excitation $f_e = 46.125$ Hz) the acoustic pressure in the pipe and the velocity of the NES. The free response in terms of acoustic pressure in the pipe considering the acoustic medium without NES is also shown. As observed in the numerical investigation, the added mass on the NES modifies the pumping characteristics. Increasing the moving mass of the NES reduces the length of the pumping phase.

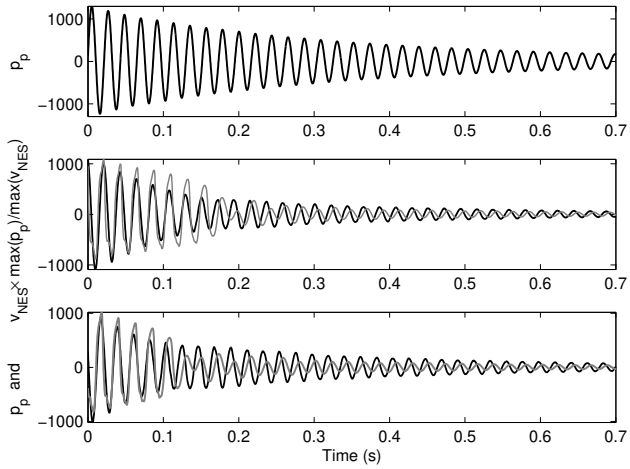


**FIGURE 10**. EXPERIMENTAL RESULTS. Time series of the pressure in the pipe (black curves) and the velocity of the diaphram of the SP NES (grey curves). Initial condition associated to the sinusoidal excitation $f_s = 46.125$ Hz and high level. Configuration without SP NES (bottom), with SP NES (middle) and with SP NES with mass (bottom).

Now, we report some forced responses under sinusoidal excitation. A constant amplitude with incremental frequency was used to analyze the behavior of the system in the frequency domain. The incremental frequency was generated by the analyzer in the frequency range $[44, 50]$ Hz with a frequency step equal to 0.125Hz. At each frequency, 32768 samples (corresponding to 8 s) of the time series were recorded. To avoid the transient part due to the unknown initial condition, only the last 2 seconds of the time trajectories were used in order to analyze the behavior of the system. At each excitation frequency and for each recorded signal, the RMS values defined as

$$RMS\, u = \sqrt{\frac{1}{T}\int_0^T u(t)^2 dt}$$

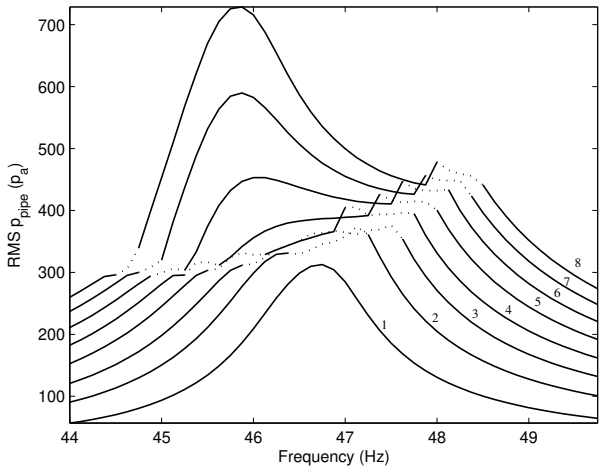


**FIGURE 11**. EXPERIMENTAL RESULTS. Configuration with SP NES without added mass. RMS of the pressure in the pipe for eight excitation amplitudes ($A_s = 0.75, 1.2, 1.6, 2., 2.4, 2.8, 3.2,$ and $3.6$). Dashed zones correspond to nonperiodic responses ($\varepsilon = 0.05$).

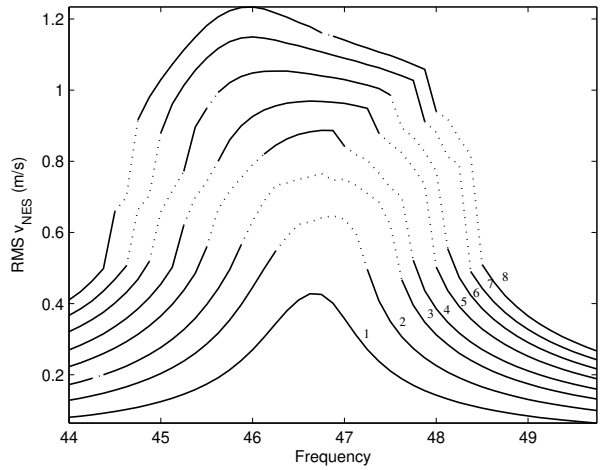


**FIGURE 12**. EXPERIMENTAL RESULTS. Configuration with SP NES without added mass. RMS of the the velocity of the diaphragm of the SP NES for eight excitation amplitudes (as in Fig. 11). Dashed zones correspond to nonperiodic responses ($\varepsilon = 0.05$).

were computed. Moreover, the following criterion

$$\frac{|\max_{k=0,\cdots,N_e}(u(kT_s)) - \min_{k=0,\cdots,N_e}(u(kT_s))|}{\max_{t\in[0,T]}|u(t)|} > \varepsilon$$

was used to detect non periodic responses associated to the sinusoidal excitation at the frequency $f_s$ ($T_s = 1/f_s$).

We consider first the SP NES without added mass. Figs. 11 and 12 show the responses in terms of acoustic pressure and velocity of the SP NES for eight excitation amplitudes. The evolution of the RMS values with the excitation level is very close to that observed with the model (see for example Fig. 11 and Fig. 7 in dimensional quantities). When the pumping appears (here for the second excitation level), the responses lose the periodic property. Still increasing the level, the resonance shifts and the periodic property is recovered.

Next, we consider the SP NES with a 3 g added mass. Fig. 13 shows the responses in terms of acoustic pressure for the same excitation amplitudes as in Fig. 11. As expected, the pumping appears for an higher excitation amplitude (here the third level).

The last result described here concerns the efficiency of the SP NES to passively reduce the noise. We consider again the SP NES without added mass and we compare it with the experimental configuration without SP NES. The results are shown in Fig. 14 in terms of RMS values of the acoustic pressure in the pipe ($p_{pipe}$), the velocity of the diaphragm of the SP NES ($v_{NES}$), the voltage and the current of the loudspeaker source. Two excitation amplitudes were used. The efficiency of the SP NES appears clearly on the RMS $p_{pipe}$ plots where the noise inside the pipe is significantly reduced. The RMS current plots show that the source loudspeaker motion is modified by the NES : beside its main role as a source, it must also be considered as a part of the primary system, even if its loose coupling does not modify

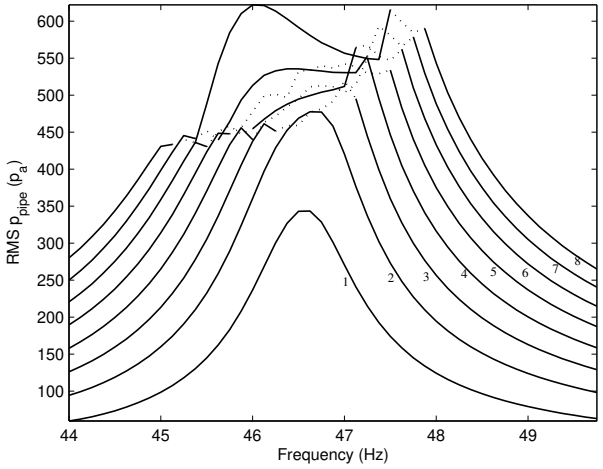


**FIGURE 13**. EXPERIMENTAL RESULTS. Configuration with SP NES with added mass (3 g). RMS of the pressure in the pipe for eight amplitude excitation levels (as in Fig. 11). Dashed zones correspond to nonperiodic responses ($\varepsilon = 0.05$).

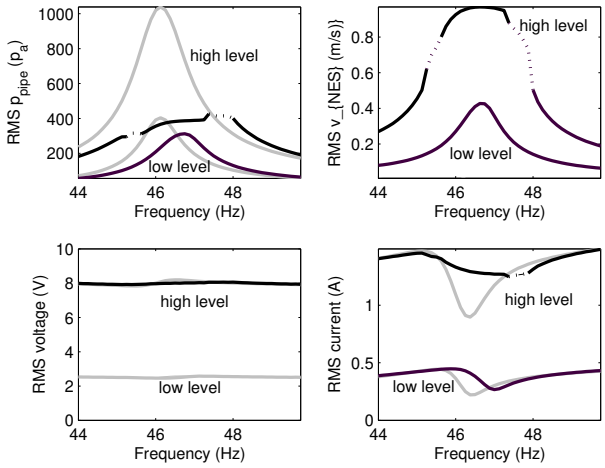


**FIGURE 14**. EXPERIMENTAL RESULTS. Configuration without NES (grey curves) and with SP NES without added mass (black curves). RMS of the pressure in the pipe ($p_{pipe}$), the velocity of the diaphragm of the SP NES ($v_{NES}$), the voltage and the current of the loudspeaker source. (Low level: $A_s = 0.75$, high level: $A_s = 2.4$). Dashed zones correspond to nonperiodic responses ($\varepsilon = 0.05$).

much the pipe resonance.

## CONCLUSION

In this paper, a more complete study of a NES based on a suspended piston technology in low frequency noise reduction context was presented. The experimental fixture considered in this work consists of a pipe (the acoustic medium) connected to a SP NES by means of a coupling box. The study has been first carried out from a simple model which is able to reproduce qualitatively the behavior of the system. The NNMs of the system have been related to forced responses under sinusoidal excitation combining the RPF representation of the NNMs and the RMS-frequency representation of the steady state responses. Experimental results have also been described. Its concern free and forced regimes. They includes the effect of the moving mass of the NES. They agree with the numerical results and the literature results, and confirm the efficiency of the SP NES to passively reduce the noise at low frequencies. The aim for further research is to develop a NES including a control of the damping by exploiting the electromagnetic circuit of the loudspeaker.

## REFERENCES

[1] Vakakis, A., Gendelman, O., Bergman, L., McFarland, D., Kerschen, G., and Lee, Y., 2008. *Nonlinear targeted energy transfer in mechanical and structural systems*, Vol. 156 of *Solid mechanics and its applications*. Springer.

[2] Gourdon, E., Alexander, N., Taylor, C., Lamarque, C.-H., and Pernot, S., 2007. "Nonlinear energy pumping under transient forcing with strongly nonlinear coupling: Theoretical and experimental results". *Journal of Sound and Vibration,* ***300***, pp. 522–551.

[3] Nucera, F., Vakakis, A., McFarland, D., Bergman, L., and Kerschen, G., 2007. "Targeted energy transfers in vibro-impact oscillators for seismic mitigation". *Nonlinear Dynamics,* ***50***, pp. 651–677.

[4] Cochelin, B., Herzog, P., and Mattei, P.-O., 2006. "Experimental evidence of energy pumping in acoustics". *C. R. Mécanique,* ***334***(11), pp. 639–644.

[5] Bellet, R., Cochelin, B., Herzog, P., and Mattei, P.-O., 2010. "Experimental study of targeted energy transfer from an acoustic system to a nonlinear membrane absorber". *Journal of Sound and Vibration,* ***329***, pp. 2768–2791.

[6] Mariani, R., Bellizzi, S., Cochelin, B., Herzog, P., and Mattei, P.-O., 2011 (to be published). "Toward an adjustable nonlinear low frequency acoustic absorber". *Journal of Sound and Vibration*.

[7] ManLab, 2010. *Version 2.0*. (http://manlab.lma.cnrs-mrs.fr/).

[8] Cochelin, B., and Vergez, C., 2009. "A high order purely frequency-based harmonic balance formulation for continuation of periodic solutions". *Journal of Sound and Vibration,* ***324***, pp. 243–262.

[9] Lazarus, A., and Thomas, O., 2010. "A harmonic-based method for computing the stability of periodic solutions". *Comptes Rendus Mcanique,* ***338***, pp. 510–517.

[10] Cochelin, B., Damil, N., and Allgowe, E., 2007. *Méthode asymptotique numrique*. Hermes Lavoisier.

## ACKNOWLEDGMENT

This research was supported by French National Research Agency in the context of the ADYNO project (ANR-07-BLAN-0193).